The Synaptojanins in the murine small and large intestine

María Dolores Vázquez-Carretero [1], Ana Eloisa Carvajal[1], José Manuel Serrano-Morales[1], Pablo García-Miranda[1], Anunciación Ana Ilundain[1], María José Peral*[1]

Abstract

The expression of the phosphoinositides phospha-tases Synaptojanins (Synjs) 1 and 2 has been shown in brain and in some peripheral tissues, but their expression in the intestine has not been reported. Herein we show that the small and large intestine express Synj1 and Synj2. Their mRNA levels, measured by RT-PCR, are not affected by development in the small intestine but in the colon they increase with age. Immunostaining assays reveal that both Synjs localize at the apical domain of the epithelial cells and at the lamina propria at sites also expressing the neuron marker calretinin. Synj2 staining at the lamina propria is fainter than that of Synj1. In colonocytes Synjs are at the apical membrane and cytosolic membrane vesicles. Synj2 is also at the mitochondria. Western blots reveal that the intestinal mucosa expresses at least two Synj1 (170- and 139-kDa) and two Synj2 (160- and 148-kDa) isoforms. The observations suggest that Synj1–170, Synj2– 160, and Synj2–148 in colonocytes, might participate in pro-cesses that take place mainly at the apical domain of the epi-thelial cells whereas Synj1–139 in those at the enteric nervous system. Experimental colitis augments the mRNA abundance of both Synjs in colon but only Synj2 mRNA levels are in-creased in colon tumors. In conclusion, as far as we know, this is the first report showing expression, location and isoforms of Synj1 and Synj2 in the small and large intestine and that they might participate in intestinal pathology.

Keywords: Synaptojanin1, Synaptojanin2, Intestine, Colon

* María José Peral mjperal@us.es

[1] Departamento de Fisiología, Facultad de Farmacia, Universidad de Sevilla, 41012 Sevilla, Spain

Introduction

Synaptojanins (Synjs) belong to a family of phosphoinositides phosphatases that have a three-domain structure: an N-terminal phosphatidylinositol polyphosphate phosphatase domain, a central inositol 5-phosphatase domain and a C-terminal pro- line-rich domain that acts primarily as a protein–protein inter- action. The domains with phosphatase activity dephosphorylate plasma membrane phosphoinositides, molecules that regulate cell proliferation and apoptosis, ionic channels and transporters, membrane vesicles traffic and cytoskeleton rearrangement, among others (Di Paolo and De Camilli 2006).

In mammals, the synaptojanin family has two members: Synj1 and Synj2, being Synj1, identified as a nerve terminal protein (McPherson et al. 1994), the best characterized. Its C-terminal region is alternatively spliced producing two main isoforms of 145- and 170-kDa, respectively (Ramjaun and McPherson 1996). The region of the C-terminal domain shared by both Synj1 isoforms interacts with proteins in- volved in clathrin-mediated endocytosis and actin organiza- tion at nerve terminals (Drouet and Lesage 2014; Billcliff and Lowe 2014). The additional C-terminal tail of Synj1–170 iso- form contains binding sites for clathrin, the clathrin adaptor AP2 and the accessory factor Eps15 (Haffner et al. 1997, 2000). Regarding tissue distribution, Synj1–145 is at very high concentrations in presynaptic nerve terminals of the adult brain, whereas Synj1–170 protein is in heart, lung, liver, testis and rat embryonic brain but undetectable in adult brain (McPherson et al. 1994; Ramjaun and McPherson 1996).

Synj2 mRNA has been detected in brain and several periph- eral tissues but it is predominantly expressed in brain, testis and cochlea (Nemoto et al. 1997, 2001; Manji et al. 2011). Synj2 undergoes alternative splicing, mostly within the C-terminal region, generating isoforms (α –ζ) in mice (Khvotchev and Südhof 1998; Seet et al. 1998) and three major isoforms in rat and human: Synj2A (140-kDa), Synj2B1 (160-kDa) and Synj2B2 (165-kDa) (Nemoto et al. 1997, 2001). Synj2A binds to the mitochondrial outer membrane protein OMP25 (Nemoto and De Camilli 1999; Nemoto et al. 2001), which is also in the cytosol and known as synaptojanin-2 binding protein (SYNJ2BP) or as activin receptor-interacting protein 2 (ARIP2). Synj2B1 and B2 lack the motif responsible for the interaction with OMP25 (Khvotchev and Südhof 1998; Seet et al. 1998) and they share with Synj1 the predominant locali- zation at nerve terminals and the interaction with endocytic proteins (Nemoto et al. 2001). Synj2B2 also interacts with pro- teins required for the formation of lamellipodia and invadopodia (Chuang et al. 2004, 2012).

Studies carried out in our laboratory revealed that rodent small intestine expresses reelin, its receptors VLDLR (very low-density lipoprotein receptor) and ApoER2 (apolipoprotein E receptor 2) and its effector protein Dab1 and that reelin par- ticipates in the homeostasis of the intestinal epithelium (García-Miranda et al., 2013; 2013). In an attempt to elucidate the signalling cascade (s) activated in response to reelin we perform binding-protein screening experiments using Dab1-coupled se- pharose beads and protein extracted from rat enterocytes. These experiments revealed that Dab1 interacts with Synj2, among other proteins (Vázquez-Carretero et al. 2012).

Since the presence of Synjs in the intestine had not been reported, as far as we were aware, we undertook a series of experiments to study their expression in the mice intestinal mucosa. Herein, we show for the first time that: i) small and large murine intestine express Synj1 and 2, ii) Synjs expres- sion shows regional differences, iii) intestinal maturation af- fects the abundance of both Synjs in the large but not in the small intestine, iv) both Synjs are located at the apical cyto- solic membrane vesicles of the epithelial cells, v) colon pa- thologies affect Synjs expression.

A preliminary report of some of these results was published as an abstract (Vázquez-Carretero et al. 2014).

Materials and methods

Chemicals

Unless otherwise indicated, the reagents used in this study were from Sigma-Aldrich, Spain. Antibodies: rabbit anti- Synj1 and rabbit anti-Synj2 for the immunohistochemistry, Western blot and immunogold electron microscopy assays were from Novus Biologicals, Littleton, CO, USA; mouse anti-Calretinin from Invitrogen Life Technologies, Carlsbad, CA, USA; mouse anti-β-Actin from Sigma-Aldrich; biotin- conjugated anti-rabbit IgG or anti-mouse IgG from Vector Laboratories, Burlingame, CA, USA; gold-conjugated anti- rabbit IgG (6 nm gold) from Aurion, The Netherlands; peroxidase-conjugated anti-rabbit IgG and peroxidase- conjugated anti-mouse IgG from Sigma-Aldrich.

Animals

20 day gestation foetuses, 15, 30, 90,120 and 300 day-old C57BL/6 mice were used. Adult rodents were fed with a nor- mal rodent diet (Harlan Ibérica S.L., Barcelona, Spain) and water ad libitum. The animals were sacrificed by cervical dis- location except the foetuses that were decapitated. Animals were humanely handled and sacrificed in accordance with the European Council legislation 86/609/EEC concerning the protection of experimental animals.

Inflammation of the colon was induced in 3 month-old mice by oral administration of 3% dextran sulphate sodium (DSS, MW 40 kDa, TdB Consultancy, Uppsala, Sweden) in the drinking water during 0, 3, 6 and 9 days as described by Cooper et al. (1993). Control mice drank normal tap water during the same period. The extent of inflammation was de- termined using established clinical and histological scoring systems. Daily throughout the DSS-treatment two observers recorded body weight loss, stool consistency and presence of blood in faeces. A score (scale of 0–3) was assigned to each of these parameters and it was utilized to calculate the average daily disease activity index (DAI) as described by Cooper et al. (1993). The grade of inflammation was evaluated by histological analysis on 5 μm paraffin embedded sections of colon stained with hematoxylin-eosin (H&E). The histologi- cal evaluations were performed in a blinded fashion by a val- idated method described by Cooper et

al. (1993) with some modifications. The parameters scored on a 0–3 scale were: destruction of epithelium and glands, dilatation of glandular crypts, depletion and loss of Goblet cells, infiltration of in- flammatory cells, edema and crypt abscesses.

Tumors were induced on 3 month-old mice following the protocol of Okayasu et al. (1996). 10 mg/kg body weight of azoxymethane (AOM) were injected intraperitoneally and 7 days later 1% DSS was administered in the drinking water during 4 days, followed by 14 days of tap water. This cycle was repeated three times. 14 days after the last cycle the mice were sacrificed. Tumors and adjacent normal tissue were extracted from the colon by microdissection. Normal tissue and tumor were evaluated by histological examination after H&E staining.

Relative quantification of real-time PCR

Total RNA was extracted from brain and mucosa of jejunum, ileum, proximal colon, distal colon and rectum of mice of different ages, using RNeasy® kit (Qiagen, Hilden, Germany). RNA purity was assessed by spectrophotometry measurements of OD260/280 and integrity by visual inspec- tion after electrophoresis on an agarose gel in the presence of ethidium bromide. cDNA was synthesized from 1 µg of total RNA using QuantiTect® reverse transcription kit (Qiagen), as described by the manufacturer. The primers for Synj1 (sense, CATAGTGGAAACTAGGCATAAGG/ antisense, CACAGA C ATGC ATC CAGTGAC), S ynj2 (sense, CTGT CTTTACATCTTTGTACGTCC/ antisense, GTCTTCAT TCCTCTCCTTCACC) and IL-β1 (sense, TTGACGGAC CCCAAAAGATG/ antisense, AGAAGGTGCTCATG TCCTCAT) were chosen according to the mice cDNA se- quences entered in Genbank and designed using PerlPrimer program v1.1.14 (Parkville, Melbourne, Victoria, Australia). Real-time PCR was performed with iQ™SYBR® Green Supermix (Bio-Rad, Hercules, CA, USA), 0.4 µM primers and 1 µl cDNA. Controls were carried out without cDNA. Amplification was run in a MiniOpticon™ System (Bio- Rad) thermal cycler (94 °C/3 min; 35 cycles of 94 °C/40 s, 58 °C/40 s, and 72 °C/40 s, and 72 °C/2 min). Following amplification, a melting curve analysis was performed by heating the reactions from 65 °C to 95 °C in 1 °C intervals while monitoring fluorescence. Analysis confirmed a single PCR product at the predicted melting temperature. The PCR primers efficiencies ranged from 90% to 110%. The cycle at which each sample crossed a fluorescence threshold, Ct, was determined and the triplicate values for each cDNA were av- eraged. Analyses of real-time PCR were done using the com- parative Ct method, with the Gene Expression Macro software supplied by Bio-Rad. β-actin (sense, CGGAACCGCTCATT GCC/ antisense, ACCCACACTGTGCCCATCTA) served as a reference gene for samples normalization. The $2^{-\Delta\Delta C}$ meth- od was used to validate β-actin as internal control gene (Livak and Schmittgen 2001).

Isolation of enterocytes and colonocytes

Enterocytes and colonocytes enriched fractions were isolated as described by Garcia-Miranda et al. (2010). Briefly, either the small or the large intestine of 30 day-old mice were rapidly removed and washed with ice-cold saline solution. 1 cm intestinal segments were incubated at room temperature in PBS buffer containing 1 mM dithiothreitol for 15 min, followed by a 30 min incubation period at 37 °C in a calcium- and magnesium-free PBS buffer containing 1 mM EDTA and 2 mM glucose. Following incubation the tissues were vortexed for 30 s, the loosened epithelial cells (enterocytes or colonocytes) were filtered through 60 µm nylon textile and collected by centrifugation and re-suspension in PBS. The isolated cells were immediately used for Western blot assays.

Immunostaining at the light microscope

Immunostaining assays were performed on intact small and large intestine of 30 day-old mice. 10 µm cryosections were incubated either with the anti-Synj1 antibody (1:50 dilution), anti-Synj2 antibody (1:25 dilution) or anti-calretinin antibody (1:100 dilution) at 4 °C, overnight. Antibody binding was visualized with biotinylated anti-rabbit IgG or anti-mouse IgG antibodies at dilution 1:100, followed by immunoperoxidase staining using the Vectastain ABC peroxidase kit (Vector Laboratories) and 3,3′-diaminobenzidine. Controls were carried out without primary antibody. The slides were mounted and photographed with a Zeiss Axioskop 40 microscope equipped with a SPOT Insight V 3.5 digital camera.

Immunostaining at the electron microscope

Segments of 3-month-old mice large intestine were fixed in 1% glutaraldehyde, 4% formaldehyde and 0.25% picric acid in 0.1 M phosphate buffer, pH 7.4, at room temperature for 3 h. After rinsing with phosphate buffer containing 3.5% sucrose (buffered sucrose), the segments were incubated for 1 h in 0.5 M ammonium chloride in buffered sucrose. Fixed tissue was dehydrated directly into 70% ethanol and embedded in LR White resin at 50 °C for 24 h using gelatin capsules. Ultrathin sections (90 nm) were mounted on nickel grids, transferred onto PBS, blocked with 0.5% BSA diluted in PBS for 15 min and incubated with the indicated antibody for 2 h at room temperature. The grids were rinsed, incubated for 1 h at room temperature with the appropriate gold conjugated secondary antibody and washed with PBS-BSA (3 × 10 min), PBS (3 × 10 min) and distilled water (3 × 10 min). Grids were stained with 2% uranyl acetate for 10 min and washed with distilled water. Controls were carried out without primary antibody. The sections were examined under a Zeiss Libra 120 Plus transmission electron microscope equipped with a TRS camera and the photographs were processed with WinTEMTM software.

Western blot assay

SDS-PAGE was performed on a 4–15% polyacrylamide gra- dient gel (TGX Stain-free precast gel, Bio-Rad) following the manufacturer's instructions. Proteins were extracted from brain, mucosa of the small and large intestine, enterocytes and colonocytes of 30 day-old mice using the following buff- er: 150 mM NaCl, 2 mM EDTA, 10 EGTA mM and 50 mM
Tris-HCl, pH 7.5, 1% Nonidet P-40, 0.1% deoxycholic acid and as proteases inhibitors: 1 mM phenylmethylsulfonyl fluo- ride, 20 µg/ml Aprotinin and 10 µg/ml Leupeptin. Protein was measured by the Bradford method (Bradford 1976) using gamma globulin as the standard. Anti-Synj1 and anti-Synj2 antibodies (1:300 dilution) were used. The dilution of the sec- ondary antibody was 1:8000. The immunoreactive bands were viewed using a chemiluminescence procedure (GE Healthcare, Little Chalfont, UK). Anti-β-actin antibody (1:4000 dilution) was used to normalize band density values. The relative abundance of the bands was quantified using ImageJ program version 1.46, National Institutes for Health (http://rsb.info.nih.gov/ij/index.html).

Statistics

Data are presented as mean ± SEM. In the figures, the vertical bars that represent the SEM are absent when they are less than symbol height. One-way ANOVA followed by Newman– Keuls´ test was used for multiple comparisons (GraphPad Prism program) and two-tailed Student's t-test for paired com- parisons. Differences were set to be significant for $p < 0.05$.

Results

Expression of *Synj1* and *Synj2* genes in mice brain and intestine

The presence in the small and large intestine of Synj1 and Synj2 mRNAs was examined by real-time RT-PCR, using total RNA extracted from the intestinal mucosa of mice of different ages. Brain was used for comparisons. The results given in Fig. 1 show that the mRNA of both Synjs is present in all the tissues examined. For both Synjs, maximal levels of their mRNA are found in brain. Synj1 mRNA levels are significantly higher than those of Synj2 in brain and small intestine, whereas the opposite is found in the large intestine. Development increases the mRNA levels of both Synjs in brain and large intestine but they either slightly decrease (Synj2) or remain more or less constant (Synj1) in the small intestine.

The plot of Synj mRNAs vs. intestinal region (Fig. 2) reveals that Synj1 mRNA abundance does not significantly vary with the intestinal region in 15 and 30 day-old mice, but it is significantly higher in the colon than in the small intestine in 4 month-old mice. Synj2 mRNA abundance in the colon is significantly greater than that in the small intestine, at all the ages tested.

Localization of synaptojanin proteins in mice small and large intestine

The localization of Synj1 and Synj2 in the intact small and large intestine was determined by immunohistochemistry at the light microscope, using antibodies against Synj1, Synj2 and calretinin. Calretinin is a calcium-binding protein abundantly expressed in neurons. Therefore, the anti-calretinin an- tibody, by staining the neural cells, will reveal the location of the enteric nervous system within the mucosa. The anti-Synj 1 and anti-Synj 2 antibodies used for these studies recognized all the Synj1 and Synj2 isoforms so far known. The results in Fig. 3 reveal that the specific signal produced by anti-Synj1 antibody is particularly strong at the terminal web domain of the enterocytes and colonocytes and in the lamina propria at sites also reactive to anti-calretinin antibody. Synj2 is detected at the terminal web domain of enterocytes and colonocytes but the staining in the lamina propria is faint. These observations indicate that both Synjs are located at the epithelial cells and that Synj1 expression in the enteric nervous system is more noticeable than that of Synj2.

As the mRNA levels of both Synjs are greater in the colon than in the small intestine, their subcellular location by immunogold electron microscopy analysis was performed only in colonocytes. Figure 4 shows that Synj1 localizes at the microvilli membrane, at the apical membrane invaginations and at cytosolic membrane vesicles. Synj2 (Fig. 5) is also located at the apical membrane between microvilli, at the endosomes and the mitochondria.

Western blot assays of intestinal Synj1 and Synj2

The above experiments are not quantitative and neither provide information on the Synjs isoforms expressed by the intestine. This was achieved by Western blot assays, using protein ex- tracted either from the mucosa, enterocytes or colonocytes of 30 day-old mice. Brain was used for comparisons.

Figure 6 shows that the anti-Synj1 antibody detects a poly- peptide of 145 kDa in brain and two of approx. 170-kDa and 139-kDa in the intestine. The Synj1–170 isoform is found in all the intestinal extracts examined whereas that of 139-kDa is excluded from both, enterocytes and colonocytes. The 170- kDa isoform is enriched by approx. 1.6-fold in the enterocytes fraction and by approx. 1.3-fold in that of colonocytes as compared with the respective mucosa.

The anti-Synj2 antibody detects polypeptides bands of approx. 124-, 148- and 160-kDa (Fig. 7). The polypeptide of approx. 124-kDa is only detected in the brain. The 160-kDa band is present in all the tissue fractions tested, being more abundant in colon (mucosa and colonocytes) followed by brain. A 10-fold enrichment in the 160-kDa band is observed in the enterocytes fraction but not in that of colonocytes as compared with the mucosa. The polypeptide band of 148-kDa is absent from the enterocytes and its abundance in the large intestine is similar to that in brain and greater than that in the mucosa of the small intestine.

Effect of either DSS- or AOM/DSS- treatment on colonic Synj1 and Synj2 abundance

As some reports have shown that Synjs are involved in peripheral pathology, we wonder whether the expression of these genes in the colon is affected by either colitis or cancer.

Experimental colitis was induced in 3 month-old mice as described in Methods. Total RNA was extracted from distal colon of untreated and DSS-treated mice and it was used for the RT-PCR assays. The development of colitis was confirmed by measuring the DAI and the pro-inflammatory cytokine IL-1β and by histological examination of the colon. The results reveal an increase in the DAI, the IL-1β mRNA levels, the loss of crypt architecture and overall structure of the lamina propria; infiltration of mixed inflammatory cells in the mucosa and submucosa; mucosal ulceration, and muscle layers thickening with the duration of the DSS-treatment (Fig. 8). Synj1 and Synj2 mRNA abundances increase at 3 and 6 days of DSS-treatment but return to basal values after 9 days of DSS-treatment even thought the inflammatory parameters measured remain high. The de- crease could result from the progressive loss of the epithelial cells produced by the inflammation.

The AOM-DSS treatment described in Methods induced tumors in all the animals and Fig. 9 shows that Synj2 mRNA abundance increased in the tumors but those of Synj1 are not affected.

Discussion

Synj1 and Synj2 have been detected at nerve terminals in brain and in some peripheral tissues but its presence in the intestine had not been reported so far. The cur-rent study demonstrates that mice small and large intestine express isoforms of both Synjs and that their ex- pression varies with intestinal region, ontogeny, DSS- induced colitis and AOM/DSS induced tumors.

In agreement with reports showing high expression of Syn1–145 isoform but no expression of the 170-kDa isoform in adult brain (Ramjaun and McPherson 1996), we found that adult mice brain exclusively expresses the Synj1–145 isoform. The intestinal mucosa expresses Synj1–170 and Synj1–139 isoforms but the latter is excluded from the epithe- lial cells. Since the immunohistochemistry assays showed Synj1 at the terminal web domain of the enterocytes and colonocytes and in the lamina propria at sites expressing calretinin, the Synj1–170 isoform might be that located at the apical domain of epithelial cells and that of 139-kDa could be that expressed by the mucosal nervous system. The lower size of this isoform compared with that in brain could be due to different degree of glycosylation.

The current results do not totally agree with previous re-ports on the molecular mass of the Synj2 isoforms. In brain we have detected three Synj2 isoforms that migrate at approximately 160-kDa, 148-kDa and 124-kDa. Planchart (2013) de tected in mice brain two Synj2 isoforms: one of 160-kDa and other of approx. 116 to120-kDa, but none of 148-kDa. Three major isoforms have been reported for rat and human in brain: Synj2A of 140-kDa, Synj2B1 of 160-kDa and Synj2B2 of 165-kDa (Nemoto et al. 1997, 2001), but none around 120-kDa, suggesting

that the 120-kDa isoform might be more abundant in mice brain than in rat. Assuming similar molecu-lar mass for the Synj2 isoforms in rat and mice, the 148-kDa isoform detected here could be Synj2A and that of 160-kDa isoform could correspond with Synj2B. Of the three isoforms detected in mice brain here, the 124-kDa isoform is absent from the intestine and the other two show intestinal region differences: the 160-kDa isoform is present in all the intestinal fractions tested and the 148-kDa isoform is not detected in the enterocytes. Therefore the 160-kDa isoform must be that detected by the immunohistochemistry at the apical domain of the enterocytes. As com-pared with the mucosa, Synj2 isoforms are enriched in the enterocytes fraction but not in that of colonocytes, although the immunohistochemistry reveals poor expression of Synj2 in the lamina propria. This apparent dis- agreement might result from the presence of Synj2 in both colonocytes and crypt cells but only colonocytes were removed from the mucosa.

The role of Synj1 in the nervous system, and to less extent that of Synj2, is well documented but Synjs expression and functions in peripheral tissues are not so well known and they are unknown in the intestine, as far as we are aware. The location of Synj1 and Synj2 in the intestine suggests their participation in processes that take place in epithelial cells and mucosal nervous sys-tem. Their functions in the enteric nervous system might be those described in brain: synaptic vesicle endocytosis and recycling (McPherson et al. 1994, 1996). Their sub- cellular location in colonocytes (at sites where the apical membrane invaginates to start endocytosis, at the cytosol membrane vesicles and at vesicles close to the cell-cell apical junctions) is consistent with a role in vesicular transport processes occurring at the apical membrane. A role of Synjs in the intestinal endocytosis of food macromolecules can be discarded because this endocytosis decreases drastically at weaning (Fujita et al. 2007) and age does not significantly modify the Synjs mRNA levels in the small intestine and increases those levels in the colon. As observed in kidney and culture cells, in the intestine Synjs might participate in the endocytosis/exocytosis of membrane proteins recycling and of molecules. In cultured cells Synj2 regulates early steps of clathrin-mediated endocytosis (Malecz et al. 2000; Hill et al. 2001; Rusk et al. 2003) and inhibits endocytosis of transferrin and epidermal growth factor receptors (Malecz et al. 2000). In kidney, Synj (the type of Synj has not been investigated) mediates the endocytosis of the apical $Na^+/K^+/2Cl^-$ co-transporter (Ares and Ortiz 2012) and Synj1–170 participates in the endocytosis of the slit diaphragm proteins (Soda et al. 2012).

The involvement of Synj2 in endocytosis may be either directly or mediated by OMP25, also known as ARIP2 or SYNJ2BP. Through this binding, Synj2–140 isoform regulates endocytosis of activin type II receptors (Matsuzaki et al. 2002), promote Delta-Notch signalling (Adam et al. 2013) and it might participate in megalin-mediated endocytosis (Gotthardt et al. 2000). Via OMP25 Synj2 also affects mitochondrial distribution and morphology (Nemoto and De Camilli 1999). Whether Synj2 controls mitochondrial distribution and morphology in the intestinal epithelium requires further investigation.

The current observations also reveal that Synjs ex- pression in the colon is

modified under pathological conditions but the modification depends on the pathology. Thus, both Synjs participate in the response of colon to inflammatory stimuli, but only Synj2 is increased in the tumors. The latter observation agrees with reports showing: i) Synj2 involvement in the formation of cell lamellipodia and invadopodia that are required for tumor cell migration and invasion (Chuang et al. 2004; Ben-Chetrit et al. 2015); ii) increased Synj2 expression in breast cancer (Ben-Chetrit et al. 2015) and in serum of patients with colorectal cancer (Lim et al. 2015), and iii) association of a Synj2 variant with colorectal cancer risk in Chinese population (Du et al. 2015).

In conclusion, as far as we know, this is the first report showing expression, location and isoforms of Synj1 and Synj2 in the small and large intestine. The observations suggest participation of Synj1–170, Synj2–160 and Synj2–148 in processes occurring at the apical domain of the epithelial cells and of Synj1–139 in those of the enteric nervous system. They also suggest their participation in the response to DSS-induced inflammation and in cancer.

Acknowledgments This work was supported by a grant from the Junta de Andalucía (CTS 05884). Electron microscope images were obtained at the Centro de Investigación, Tecnología e Innovación de la Universidad de Sevilla (CITIUS).

References

Adam MG, Berger C, Feldner A, Yang WJ, Wüstehube-Lausch J, Herberich SE, Pinder M, Gesierich S, Hammes HP, Augustin HG, Fischer A (2013) Synaptojanin-2 binding protein stabilizes the notch ligands DLL1 and DLL4 and inhibits sprouting angiogenesis. Circ Res 113:1206–1218

Ares GR, Ortiz PA (2012) Dynamin2, clathrin, and lipid rafts mediate endocytosis of the apical Na/K/2Cl cotransporter NKCC2 in thick ascending limbs. J Biol Chem 287:37824–37834

Ben-Chetrit N, Chetrit D, Russell R, Körner C, Mancini M, Abdul-Hai A, Itkin T, Carvalho S, Cohen-Dvashi H, Koestler WJ, Shukla K, Lindzen M, Kedmi M, Lauriola M, Shulman Z, Barr H, Seger D, Ferraro DA, Pareja F, Gil-Henn H, Lapidot T, Alon R, Milanezi F, Symons M, Ben-Hamo R, Efroni S, Schmitt F, Wiemann S, Caldas C, Ehrlich M, Yarden Y (2015) Synaptojanin 2 is a druggable mediator of metastasis and the gene is over expressed and amplified in breast cancer. Sci Signal 8(360):ra7

Billcliff PG, Lowe M (2014) Inositol lipid phosphatases in membrane trafficking and human disease. Biochem J 461:159–175

Bradford MM (1976) A rapid and sensitive method for the quantification microgram quantities of protein utilizing the principle of protein dye binding. Anal Biochem 72:248–254

Chuang YY, Tran NL, Rusk N, Nakada M, Berens ME, Symons M (2004) Role of synaptojanin 2 in glioma cell migration and invasion. Cancer Res 64:8271–8275

Chuang Y, Xu X, Kwiatkowska A, Tsapraillis G, Hwang H, Petritis K, Flynn D, Symons M (2012) Regulation of synaptojanin 2 5'-phos- phatase activity by Src. Cell Adhes Migr 6:518–525

Cooper HS, Murthy SN, Shah RS, Sedergran DJ (1993) Clinicopathologic study of dextran sulfate sodium experimental mu- rine colitis. Lab Investig 69:238–249

Di Paolo G, De Camilli P (2006) Phosphoinositides in cell regulation and membrane dynamics. Nature 443:651–657

Drouet V, Lesage S (2014) Synaptojanin 1 mutation in Parkinson's dis- ease brings further insight into the neuropathological mechanisms. Biomed Res Int 2014(289728):1–9

Du Q, Guo X, Zhang X, Zhou W, Liu Z, Wang J, Zhang T, Mao Z, Luo J, Jin T, Liu C (2015) SYNJ2 variant rs9365723 is associated with colorectal cancer risk in Chinese Han popu- lation. Int J Biol Markers 28 31(2):e138–e143. doi:10.5301/jbm.5000182

Fujita M, Baba R, Shimamoto M, Sakuma Y, Fujimoto S (2007) Molecular morphology of the digestive tract; macromolecules and food allergens are transferred intact across the intestinal absorptive cells during the neonatal suckling period. Med Mol Morphol 40:1–7

Garcia-Miranda P, Peral MJ, Ilundain AA (2010) Rat small intestine expresses the reelin-disabled-1 signalling pathway. Exp Physiol 95:498–507

García-Miranda P, Vázquez-Carretero MD, Sesma P, Peral MJ, Ilundain AA (2013) Reelin is involved in the crypt-villus unit homeostasis. Tissue Eng Part A 19:188–198. doi:10.1089/ten. TEA.2012.0050

Gotthardt M, Trommsdorff M, Nevitt MF, Shelton J, Richardson JA, Stockinger W, Nimpf J, Herz J (2000) Interactions of the low density lipoprotein receptor gene family with cytosolic adaptor and scaffold proteins suggest diverse biological functions in cellular communication and signal transduction. J Biol Chem 275:25616–25624

Haffner C, Takei K, Chen H, Ringstad N, Hudson A, Butler MH, Salcini AE, Di Fiore PP, De Camilli P (1997) Synaptojanin 1: localization on coated endocytic intermediates in nerve terminals and interaction of its 170 kDa isoform with Eps15. FEBS Lett 419:175–180

Haffner C, Di Paolo G, Rosenthal JA, de Camilli P (2000) Direct interaction of the 170 kDa isoform of synaptojanin 1 with clathrin and with the clathrin adaptor AP-2. Curr Biol 10: 471–474

Hill E, van Der Kaay J, Downes CP, Smythe E (2001) The role of dynamin and its binding partners in coated pit invagination and scission. J Cell Biol 152:309–323

Khvotchev M, Südhof TC (1998) Developmentally regulated al- ternative splicing in a novel synaptojanin. J Biol Chem 273: 2306–2311

Lim LC, Looi ML, Syed Zakaria SZ, Sagap I, Rose IM, Chin SF, Jamal R (2015) Identification of differentially expressed proteins in the se- rum of colorectal cancer patients using 2D-DIGE proteomics anal- ysis. Pathol Oncol Res 22:169–177

Livak KJ, Schmittgen TD (2001) Analysis of relative Gene expression data using real-time quantitative PCR and the $2^{-\Delta\Delta C_T}$ method. Methods 25:402–408

Malecz N, McCabe PC, Spaargaren C, Qiu R, Chuang Y, Symons M (2000) Synaptojanin 2, a novel Rac1 effector that regulates clathrin-mediated endocytosis. Curr Biol 10:1383–1386

Manji SS, Williams LH, Miller KA, Ooms LM, Bahlo M, Mitchell CA, Dahl HH (2011) A mutation in synaptojanin 2 causes progressive hearing loss in the ENU-mutagenised mouse strain Mozart. PLoS One 6:e17607

Matsuzaki T, Hanai S, Kishi H, Liu Z, Bao Y, Kikuchi A, Tsuchida K, Sugino H (2002) Regulation of endocytosis of activin type II receptors by a novel PDZ protein through Ral/ Ral-binding protein 1-dependent pathway. J Biol Chem 277: 19008–19018

McPherson PS, Takei K, Schmid SL, De Camilli P (1994) P145, a major Grb2-binding protein in brain, is colocalized with dynamin in nerve terminals where it undergoes activity dependent dephosphorylation. J Biol Chem 269:30132–30139

McPherson PS, Garcia EP, Slepnev VI, David C, Zhang X, Grabs D, Sossin WS, Bauerfeind R, Nemoto Y, De Camilli P (1996) A presynaptic inositol-5-phosphatase. Nature 379: 353–357

Nemoto Y, De Camilli P (1999) Recruitment of an alternatively spliced form of synaptojanin 2 to mitochondria by the interaction with the PDZ domain of a mitochondrial outer membrane protein. EMBO J 18:2991–3006

Nemoto Y, Arribas M, Haffner C, De Camilli P (1997) Synaptojanin 2, a novel synaptojanin isoform with a distinct targeting domain and expression pattern. J Biol Chem 272: 30817–30821

Nemoto Y, Wenk MR, Watanabe M, Daniell L, Murakami T, Ringstad N, Yamada H, Takei K, De Camilli P (2001) Identification and charac- terization of a synaptojanin 2 splice isoform predominantly expressed in nerve terminals. J Biol Chem 276:41133–41142

Okayasu I, Ohkusa T, Kajiura K, Kanno J, Sakamoto S (1996) Promotion of colorectal neoplasia in experimental murine ulcerative colitis. Gut 39:87–92

Planchart A (2013) Analysis of an intronic promoter within Synj2. Biochem Biophys Res Commun 440:640–645

Ramjaun AR, McPherson PS (1996) Tissue-specific alternative splicing generates two synaptojanin isoforms with differential membrane binding properties. J Biol Chem 271:24856–24861

Rusk N, Le PU, Mariggio S, Guay G, Lurisci C, Nabi IR, Corda D, Symons M (2003) Synaptojanin 2 functions at early step of clathrin-mediated endocitosis. Curr Biol 13:659–663

Seet LF, Cho S, Hessel A, Dumont DJ (1998) Molecular cloning of multiple isoforms of synaptojanin 2 and assignment of the gene to mouse chromosome 17A2-3.1. Biochem Biophys Res Commun 247:116–122

Soda K, Balkin DM, Ferguson SM, Paradise S, Milosevic I, Giovedi S, Volpicelli-Daley L, Tian X, Wu Y, Ma H, Son SH, Zheng R, Moeckel G, Cremona O, Holzman LB, De Camilli P, Ishibe S (2012) Role of dynamin, synaptojanin, and endophilin in podocyte foot processes. J Clin Invest 122:4401–4411

Vázquez-Carretero MD, García-Miranda P, Calonge ML, Calvo E, Lopez JA, Romero F, Ilundain AA, Peral MJ (2012) Disabled-1 protein in the intestine. Genes Nutr 6:S75 (meeting abstract)

Vázquez-Carretero MD, Palomo M, Carvajal AE, Serrano-Morales JM, Calonge ML, Ilundain AA, Peral MJ (2014) Synaptojanins expres-sion in the small and large intestine. Acta Physiol 212(698):90 (meeting abstract)

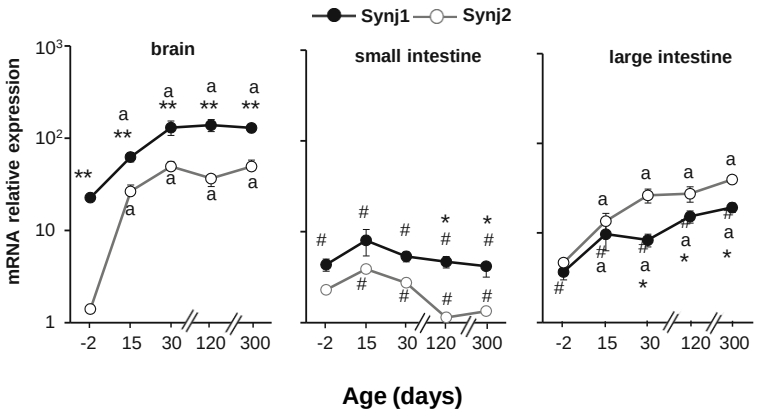

Fig. 1 Age-dependent Synj1 and Synj2 mRNA abundance in the intestine and brain. RT-PCR was performed on total RNA isolated from brain and from the mucosa of the small intestine and colon. Fetuses, 15, 30, 120 and 300 day-old mice were used. The Synj2 mRNA abundance measured in the small intestine of 120 day-old mice was set at 1. The values represent means ± SEM of arbitrary units of mRNA levels and are plotted on a logarithmic scale. Four animals were used in each condition. One-way ANOVA showed an effect of maturation on Synj1 and Synj2 mRNA levels ($p < 0.001$). Newman-Keuls´ test: #$p < 0.05$ as compared with brain, $^{a}p < 0.05$ as compared with fetuses, $^{b}p < 0.05$ and $^{bb}p < 0.001$ vs. jejunum, *$p < 0.05$ and **$p < 0.001$ Synj1 vs. Synj2.

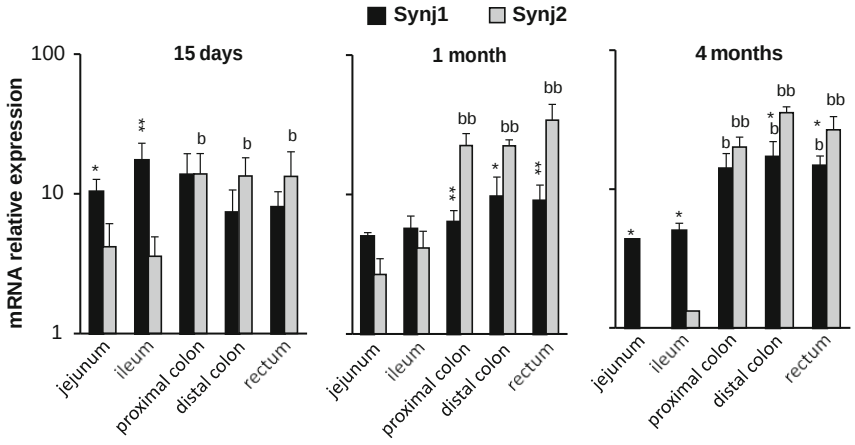

Fig. 2 Synj1 and Synj2 mRNA abundance along the intestine. Mucosa either of jejunum, ileum, proximal colon, distal colon or rectum of 0.5, 1, and 4 month-old mice was used. Synj2 mRNA abundance measured in the jejunum of 4 month-old mice was set at 1. The values represent means ± SEM of arbitrary units of mRNA levels and are plotted on a logarithmic scale. Four animals were used in each condition. One-way ANOVA showed an effect of intestinal region on Synj1 and Synj2 mRNA levels ($p < 0.001$). Newman–Keuls´ test: bp < 0.05 and bbp < 0.001 vs. jejunum,*p < 0.05 and **p < 0.001 Synj1 vs. Synj2

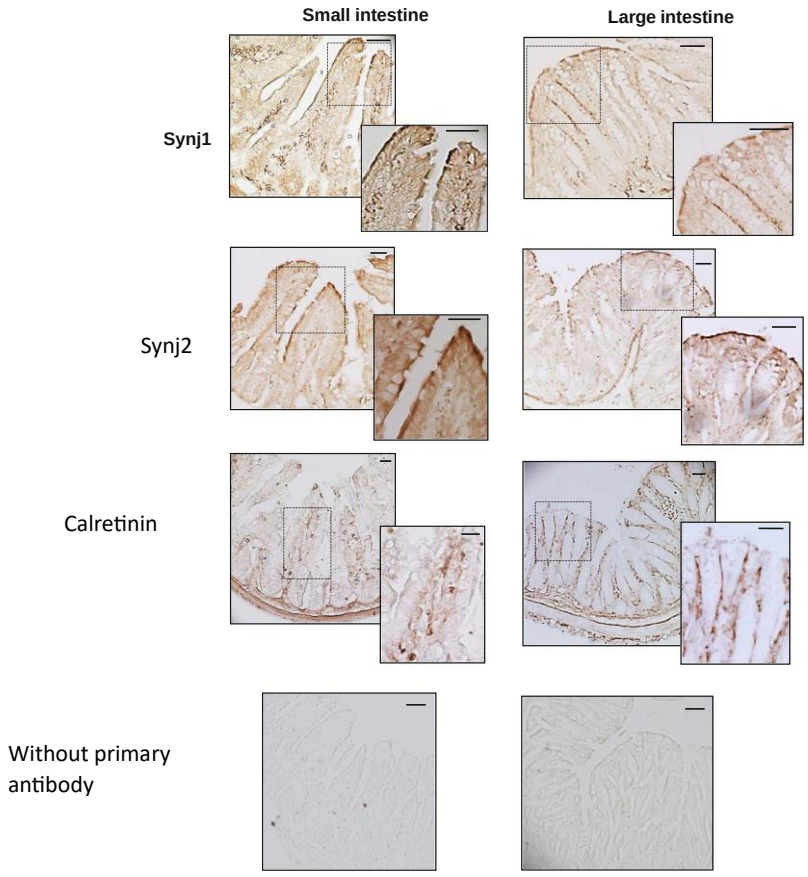

Fig. 3 Immunolocalization of Synj1, Synj2 and calretinin in the small and large intestine at the light microscope. 10 µm intestinal cryosections of small and large intestine were incubated either with anti-Synj1 (1:50 dilution), anti- Synj2 (1:25 dilution) or anti- calretinin (1:100 dilution) antibodies. Scale bars represent 50 µm. The photographs are representative of four different assays. 1 month-old mice were used.

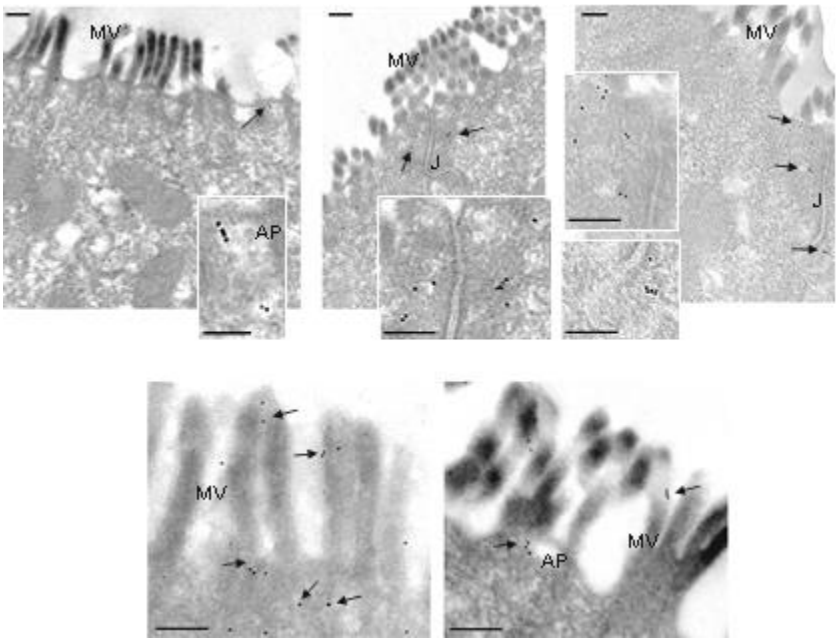

Fig. 4. Immunolocalization of Synj1 in the epithelium of mouse microscope. The distal colon of 3- month-old mice was used. The dilution of the anti-Synj1 antibody was 1:10 and that of the rabbit anti- IgG was 1:30. Immunogold labeling of Synj1 (6 nm) is indicated by arrows. The photographs show staining at microvilli (MV), apical pits (AP) and junctions (J) of four different assays. Scale bar represents 100 nm.

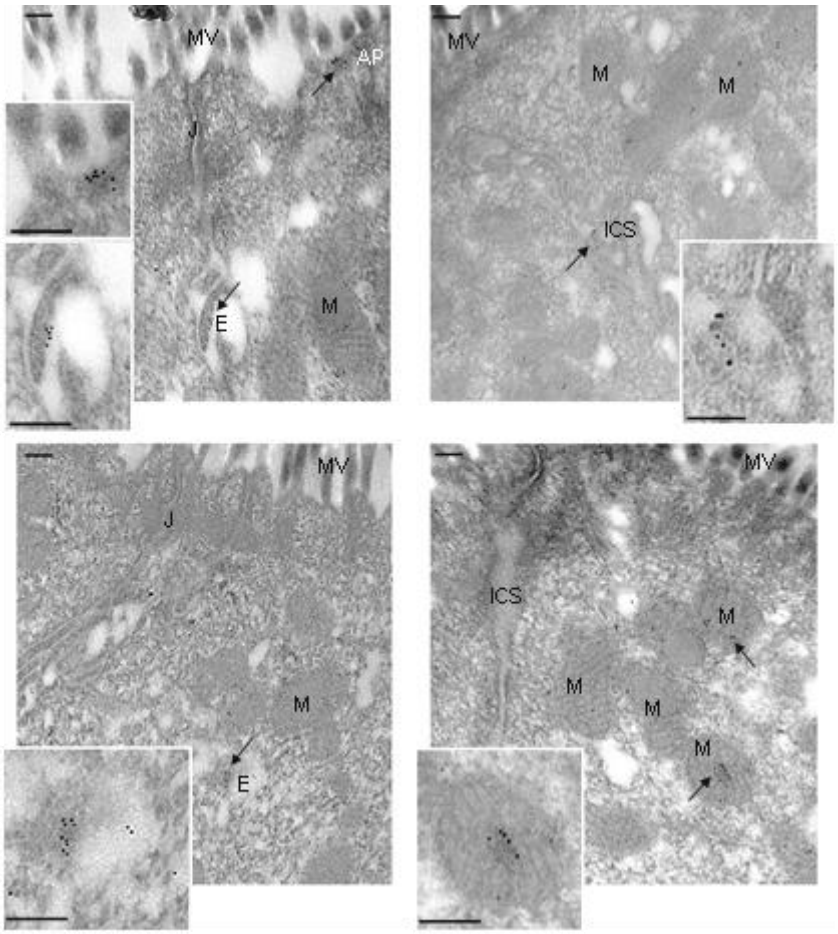

Fig. 5 Immunolocalization of Synj2 in the epithelium of mouse distal colon at the electron microscope. The distal colon of 3- month-old mice was used. The dilution of the anti-Synj2 antibody was 1:10 and that of the rabbit anti-IgG was 1:30. Immunogold labeling of Synj2 (6 nm) is indicated by arrows. The photographs show staining at intercellular space (ICS), apical pits (AP), endosomes (E) and mitochondria (M) of four different assays. Scale bar represents 100 nm.

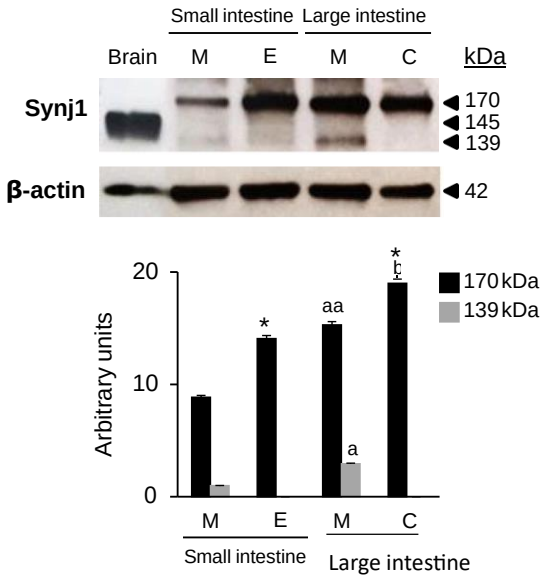

Fig. 6 Western blot of Synj1. Protein extracts of the intestinal mucosa (M), enterocytes (E), colonocytes (C) and brain were obtained from 30 day-old mice. Either 70 µg of intestinal protein or 1 µg of protein for brain were loaded per lane. The blots were probed with a commercial polyclonal anti-Synj1 antibody (1:300 dilution). Histograms represent the relative abundance of Synj1 in the intestinal extracts. Means ± SEM. ANOVA showed an effect of either the intestinal region or the mucosal location on Synj1 abundance ($p < 0.001$). Newman Keuls'test: $^{a}p < 0.05$ and $^{aa}p < 0.001$ colon mucosa vs. small intestinal mucosa, $^{b}p < 0.001$ colonocytes vs. enterocytes, $*p < 0.001$ cells extracts vs. mucosa extracts. The blot is representative of four Western blots.

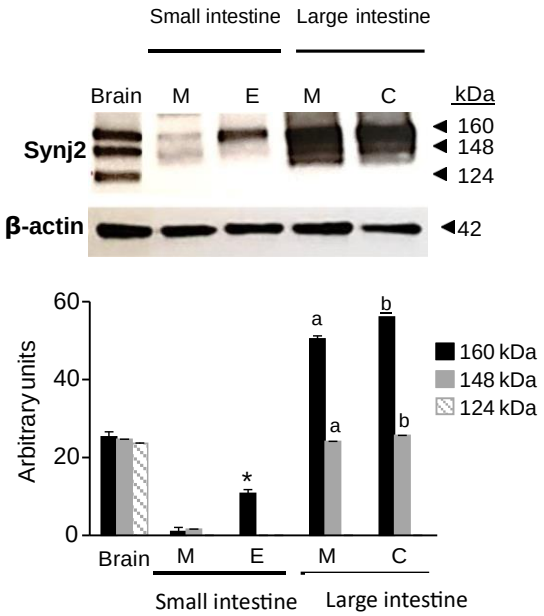

Fig. 7 Western blot of Synj2. 70 µg of protein were loaded per lane. The blots were probed with a commercial polyclonal anti-Synj2 antibody (1:300 dilution). Histograms represent the relative abundance of Synj2 in the intestinal extracts. Means ± SEM. ANOVA showed an effect either the intestinal region or the mucosal location on Synj2 isoforms abundance ($p < 0.001$). Newman Keuls'test: $^{a}p < 0.001$ colon mucosa vs. small intestinal mucosa, $^{b}p < 0.001$ colonocytes vs. enterocytes, $*p < 0.001$ cells extracts vs. mucosa extracts. The blot is representative of four Western blots. Other details as in Fig. 6

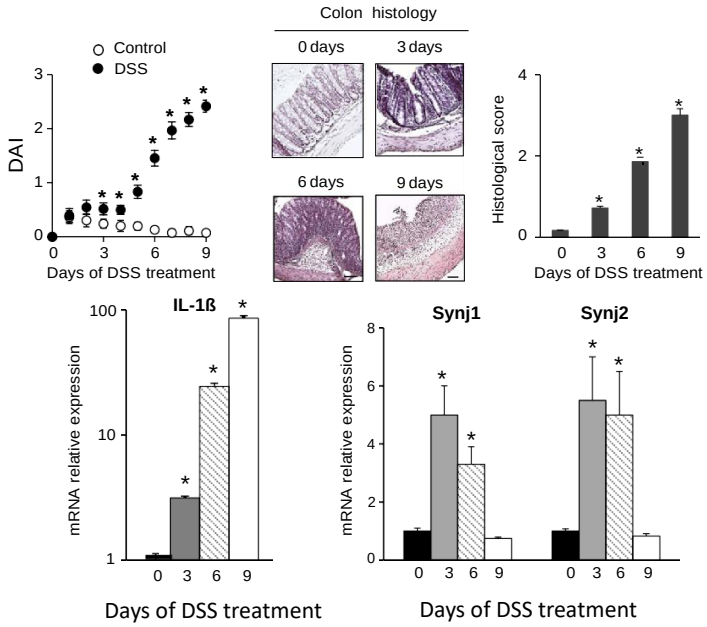

Fig. 8 Synj1 and Synj2 mRNA abundance in distal colon of DSS-treated mice. 3 month-old mice were given either water or water containing 3% DSS during 0, 3, 6 and 9 days to induce experimental colitis. The DAI, IL-1ß mRNA levels and representative H&E stained sections are the inflammatory parameters evaluated. The abundance of either IL-1ß, Synj1 or Synj2 mRNA measured in control mice was set at 1. Values represent means ± SEM of arbitrary units of mRNA levels. The photographs are representative of four different assays. Scale bar represents 100 µm. Four animals were used. Student's t test: *$p < 0.001$ colitis vs. control

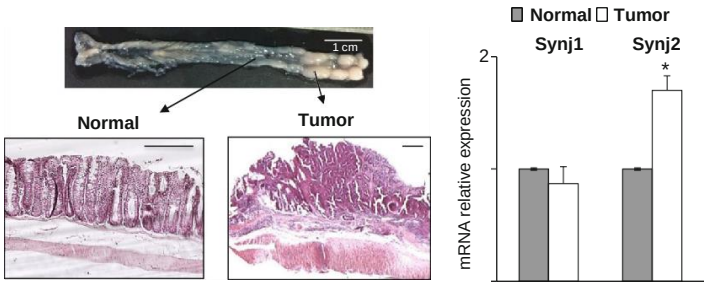

Fig. 9 Synj1 and Synj2 mRNA abundance in distal colon of AOM/DSS-treated mice. 3 month-old mice received intraperitoneal administration of AOM followed by oral administration of DSS in the drinking water, as described in Methods. Representative macroscopic view of colon and H&E stained sections showing normal tissue adjacent to the tumor and tumor. The abundance of either Synj1 or Synj2 mRNA measured in normal colon adjacent to the tumor was set as 1. Values represent means ± SEM of arbitrary units of mRNA levels. The photographs are representative of four different assays. Scale bar represents 100 μm. Four animals were used. Student's t test: $*p < 0.05$ tumor vs. normal tissue